Macromolecules
ARTICLE

Macromolecules **2009**, *42*, 6543–6548 **6543**
DOI: 10.1021/ma9011686

Synthesis of Polyoxometalate–Polymer Hybrid Polymers and Their Hybrid Vesicular Assembly

Yaokun Han,[†] Yu Xiao,[†] Zijian Zhang,[†] Bo Liu,[†] Ping Zheng,[†] Shangjin He,[‡] and Wei Wang*,[†]

[†]*The Key Laboratory of Functional Polymer Materials and Institute of Polymer Chemistry, College of Chemistry, Nankai University, Tianjin 300071, China, and* [‡]*Department of Chemistry, College of Chemistry, Nankai University, Tianjin 300071, China*

Received May 31, 2009; Revised Manuscript Received July 17, 2009

ABSTRACT: An organic–inorganic hybrid polymer composed of a Dawson trivanadium-substituted heteropolytungstate ($(Bu_4N)_5[H_4P_2W_{15}V_3O_{62}]$) cluster and PS chain are originally designed and first synthesized via in situ ATRP. Further characterization includes NMR spectroscopy, FT-IR spectroscopy, and GPC which proved the purity of the material. By means of a cation exchange process, a hybrid polymer $(Bu_4N)^+$-POM-PS was tuned into a novel giant amphiphile H^+-POM-PS. Immediately, individual molecules self-assembled into kinetically favored hybrid vesicles in DMF. Our work provides a controllable and rational way to fabricate stable and well-defined POM–polymer hybrid polymers that can be optimized for potential applications.

Introduction

Polyoxometalates (POMs, for convenience) is a class of well-known molecularly defined, discrete and anionic metal–oxygen clusters of early transition metals in their highest oxidation states (most commonly V^V, Mo^{VI}, and W^{VI}).[1,2] In the past decades, POM macroanions have attracted considerable interest because of their widespread use in many fields including catalysis, magnetism, medicinal chemistry, and materials science. In recent years, the bioactivity of POMs have been increasingly recognized,[3,4] and their applications as drugs against HIV[5,6] and cancer[7,8] are becoming a key topic. In contrast to their intriguing functionality, however, the poor compatibility of POMs with other materials and the poor processability as inorganic crystalline or powdered materials are severely limiting their potential utilization. Therefore, the development of suitable methods and technologies to modify and then utilize POMs has become a focus topic. Indeed, great efforts have been devoted in developing novel organic–inorganic hybrid materials by means of electrostatic interactions between POM anions and other organic counterions[9−13] or by means of covalent linkages of organic groups into the POM framework (or organically derived POMs).[14−18] The main purpose of these works is to enhance the functionality of macroanions through inlaying them in the specified nanostructures. Since the covalent link significantly improves the stability of the hybrid and might enhance the interaction between the inorganic and organic components, there is clearly a need for the development of covalent approach. Nevertheless, the construction of such materials represents a considerable synthetic challenge yet, and only a few methods are highly efficient and specific, especially for covalently linked POMs. This is not surprising in consideration of the difficulty met in combining inorganic POMs with organic motifs together. Nowadays, incorporation of tris(hydroxymethyl)methane derivatives onto POMs has proven to be an viable route to develop organic–inorganic hybrid POMs.[19−22] Our interest lies in the area of constructing a class of novel POM-functionalized materials that can be optimized for potential applications. Thus, as part of our efforts to manipulate a class of novel hybrid materials based on polyoxometalates and conventional polymers, we wish to develop a controllable and rational way to create stable, well-defined POM-containing hybrid materials under mild reaction conditions.

Because of its tolerance to a wide range of functional monomers and less rigorous reaction conditions, atom transfer radical polymerization (ATRP) has been one of the most frequently used technique in the synthesis of linear polymers and copolymers with a predetermined degree of polymerization (DP) and relatively narrow molecular weight distribution.[23−25] Apart from this, the preserved terminal halogen atom(s) of the polymers produced by ATRP can be successfully converted into various desired functional chain-end groups through appropriate transformations. In this work, such synthesis strategy was adopted: polymerizable groups were grafted onto the reactive sites of POMs through a covalent linkage. POM derivatives, therefore, were further used as a macroinitiator and then initiated ATRP of polystyrene.

Herein, we report the synthesis of an organic–inorganic hybrid polymer composed of a Dawson trivanadium-substituted heteropolytungstate ($(Bu_4N)_5[H_4P_2W_{15}V_3O_{62}]$) and conventional PS chain via in situ ATRP as an efficient method to generate well-defined POM–polymer hybrid materials. To the best of our knowledge, this is the first report of the synthesis of POM–polymer hybrid polymer that was initiated by in situ ATRP. Moreover, hybrid polymer $(Bu_4N)^+$-POM-PS was tuned into a giant amphiphile H^+-POM-PS through protonation. Then the formation of the hybrid vesicular assembly of the hybrid polymer was characterized by transmission electron microscopy.

Results and Discussion

A. POM Macroinitiator Design and Synthesis. To achieve our goal, we have synthesized the Dawson trivanadium-substituted heteropolytungstate ($(Bu_4N)_5[H_4P_2W_{15}V_3O_{62}]$) cluster, according to the method reported in ref 26. Three-dimensional structure of a targeted $(Bu_4N)^+$-POM-PS hybrid polymer is presented in both polyhedral and ball and stick mode in Figure 1. The negatively charged POM cluster is covered by five tetrabutylammonium (Bu_4N^+)

*Corresponding author. E-mail: weiwang@nankai.edu.cn.

Published on Web 07/24/2009

Scheme 1. Preparation of POM Macroinitiator and Its POM−PS Hybrid Polymer via ATRP

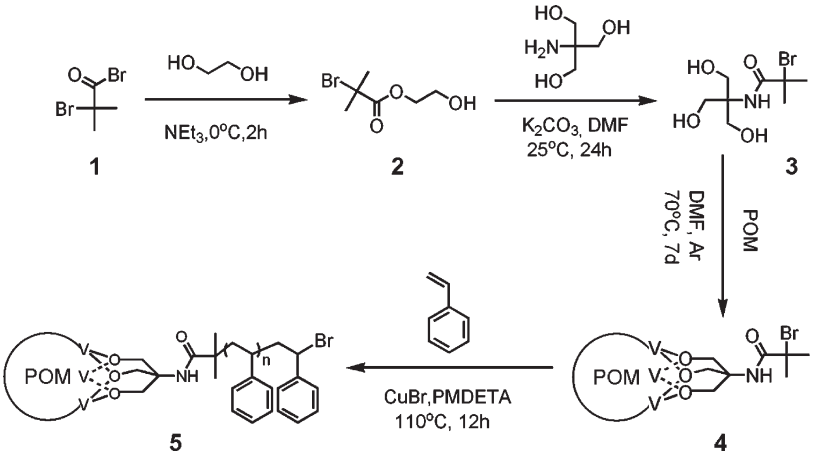

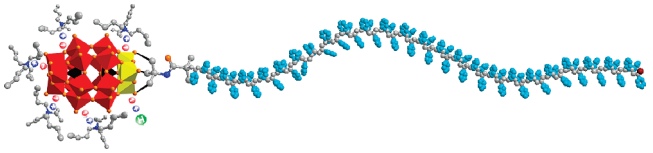

Figure 1. Three-dimensional structure of $(Bu_4N)^+$-POM-PS hybrid polymer. The inorganic and organic parts are presented in a polyhedral mode and ball and stick mode, respectively (P, black; W, red; V, yellow; O, orange; H, green; N, blue; C, gray; benzene ring, cyan; Br, brown).

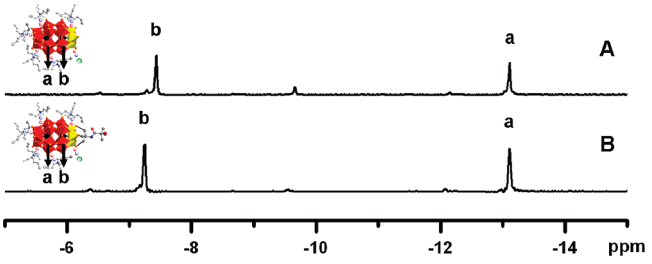

Figure 2. ^{31}P NMR spectra of (A) $(Bu_4N)_5[H_4P_2W_{15}V_3O_{62}]$ and (B) compound **4** in CD_3CN (P, black; W, red; V, yellow; O, orange; H, green; N, blue; C, gray; Br, brown).

counterions and one proton (H^+). The major reason that we select this cluster is that it is a representative redox and catalytically active POM and can be performed an organic modification by replacing the oxygen atoms bridging the vanadium atoms with methoxy groups.[20] As a straightforward example to demonstrate the concept, $(Bu_4N)^+$-POM-PS prepared via in situ ATRP (Scheme 1) was chosen as the model. Compound **2** were converted to the desired compound **3** by reaction with tris(hydroxymethyl)aminomethane (Tris) in *N,N*-dimethylformamide (DMF) at 70 °C via the previously described procedure;[27,28] however, purification of the products proved extremely difficult. Similar solubility of **3** and Tris made separation by precipitation impossible; thus, **3** was purified by passing through a silica gel column. The obtained new compound **3** has dual reactivity: one side of the compound can be covalently linked to the POM cluster; the other side can initiate a living radical polymerization of common alkene monomers, such as styrene. The esterification of POM with **3** in dry organic polar aprotic solvents is demonstrated to be efficient and convenient by replacing the oxygen atoms bridging the vanadium atoms in the V_3 "cap" of this POM with methoxy groups. The high-sensitivity ^{31}P NMR spectrum, Figure 2A, shows two main types of phosphorus resonances, expected for $(Bu_4N)_5[H_4P_2W_{15}V_3O_{62}]$ cluster. The peaks at −13.11 and −7.44 ppm are assigned to the PO_4^{3-} groups connected to the W_3 cap and V_3 cap, respectively. The shift of the peak from −7.44 to −7.25 ppm in Figure 2B is caused by the esterification of POM with **3**. Thus, successful synthesis of the POM macroinitiator was further supported by ^{31}P NMR spectra.

B. Synthesis of Bu_4N^+-POM-PS via ATRP. As shown in Scheme 1, compound **4**, the POM macroinitiator, with the bromide group initiated a polymerization of styrene monomer to create the first Bu_4N^+-POM-PS hybrid polymer, **5**, via in situ ATRP. The POM head has a fixed size and ellipsoid-like shape with 1.12 nm in diameter and 1.33 nm in length, whereas the long PS tail has a coil chain conformation and an adjustable length that can be manipulated by controlling the degree of polymerization ($\overline{DP}_n$). The hybrid polymer used here for the further study, we have $\overline{M}_n = 86\,000$ g/mol for the PS block and $M = 5180$ g/mol for the POM cluster. The success of the polymerization was further supported by evidence from ^1H NMR, FTIR, and GPC spectrometry. Hybrid polymer **5** exhibited the characteristic resonances of protons both in polystyrene (1.2−2.2 ppm (m, aliphatic main chain), 6.4−7.4 ppm (m, 5H, aromatic)) and near the terminal POM unit (5.6−5.8 ppm) in ^1H NMR spectra in Figure 3C. FTIR spectra in Figure 4C confirmed the stability of the resulting POM polymer. FTIR bands (KBr disk): 1083.9, 951, 909, 820 cm^{-1} (polyoxometalate region); C−H str (3000−3100 cm^{-1}), C=C str (1450−1600 cm^{-1}), 5 adj H wag. (755 cm^{-1}), ring wag. (699 cm^{-1}) from the aromatic rings and C−H str (ca. 2900 cm^{-1}) from the alkyl portion (PS region).

To explore the properties and understand the nature of POM−polymers, we need model compounds that have 100% POM functionality and well-defined structure. The POM−polymer hybrid polymer, we obtained, could serve as an excellent model compound. Sometimes, it can exhibit significantly different behavior and be more useful than those contaminated by impurities. Both the molecular weights of Bu_4N^+-POM-PS ($\overline{M}_n$ = 119 000) and its PS segment ($\overline{M}_n$ = 86 000) obtained by etching the Bu_4N^+-POM-PS hybrid polymer by KOH in DMF were determined by GPC, as shown in Figure 5. As expected, the samples gave a unimodal, symmetric peak. The clear shift of the GPC peak to the longer elution time (lower molecular weight) region in Figure 5 indicates the successful polymerization, confirming the cleanliness of the reaction and the 100% POM functionality of the resulting hybrid polymers. Considering the molecular weight of the POM cluster (5180), the

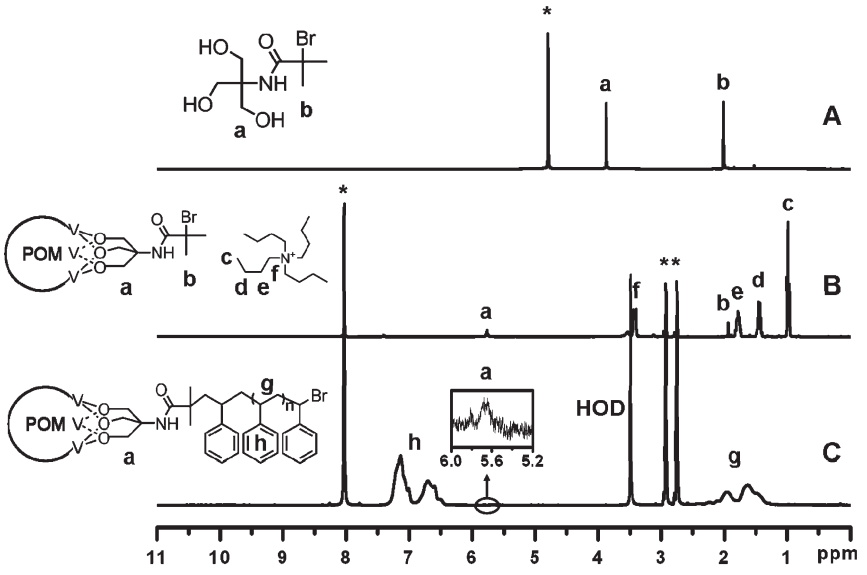

Figure 3. ^{1}H NMR spectra of (A) compound **3** in D_2O (* the peak of D_2O), (B) compound **4** in d_7-DMF (* the peak of d_7-DMF), and (C) compound **5** in d_7-DMF (* the peak of d_7-DMF).

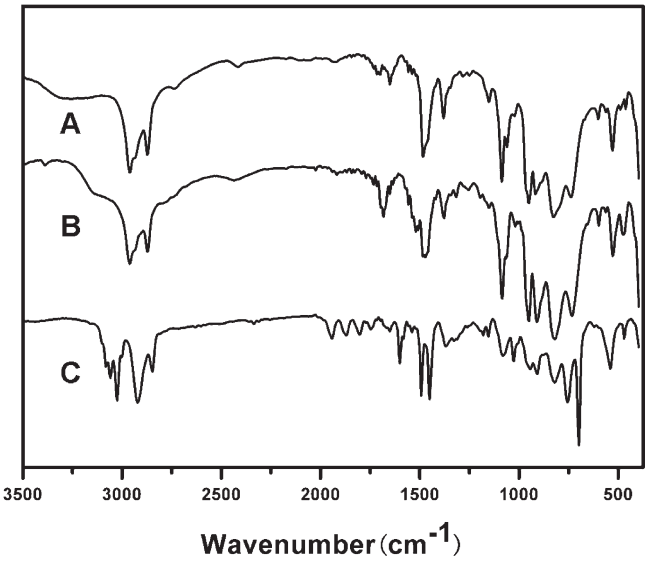

Figure 4. IR spectra of (A) $(Bu_4N)_5[H_4P_2W_{15}V_3O_{62}]$, (B) compound **4**, and (C) compound **5** taken as KBr disks.

large difference of the molecular weight between the POM-functionalized polymer and its PS segment reveals that the POM head significantly increases the overall hydrodynamic volume of the POM−PS polymer. Therefore, we hypothesize that the POM cluster has profound effects on the morphology of supramolecular assemblies of the hybrid polymer. These results unambiguously support the structure, uniformity, and purity of the hybrid polymer obtained. It was also found that the hybrid polymer was pretty stable contrary to literature reports that the POM, we used here, was routinely protected from light.[26] It can be handled without special caution to be protected from light, O_2, and moisture. No obvious decomposition is observed after its solution stand in air for nearly one month. The facile reaction and purification along with the high efficiency make it particularly useful when the materials to be functionalized can be covalently linked to the polymerizable groups.

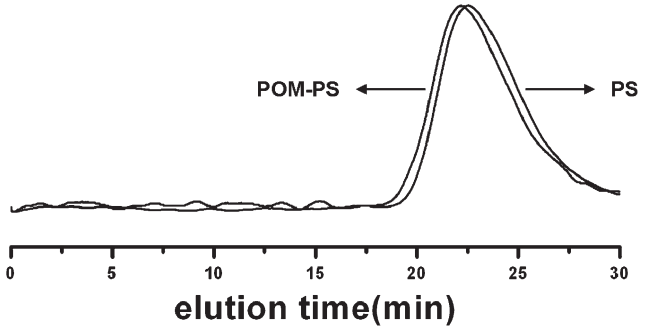

Figure 5. GPC chromatograms of $(Bu_4N)^+$-POM-PS hybrid polymer ($\overline{M}_n$ = 119 000) and its PS segment ($\overline{M}_n$ = 86 000) obtained by etching the $(Bu_4N)^+$-POM-PS hybrid polymer by KOH in DMF.

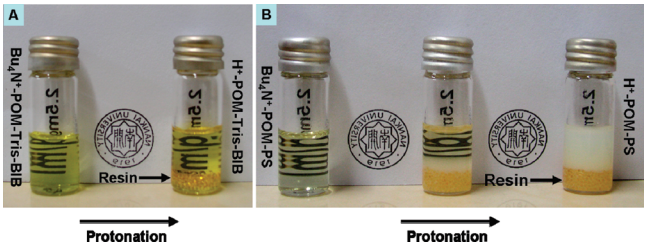

Figure 6. Digital photographs of (A) $(Bu_4N)^+$-POM-Tris-BIB in DMF and after the H^+-resin was added. (B) $(Bu_4N)^+$-POM-PS in DMF and after the H^+-resin was added.

C. Procedure for Amphiphilic H^+-POM-PS and the Hybrid Vesicular Assembly. Because of a good solubility of the Bu_4N^+-POM macroinitiator and Bu_4N^+-POM-PS hybrid polymer, their solution in DMF are transparent at a concentration of 2.5 mg mL^{-1}. Once a small amount of Dowex H^+ 50W-X2 resin is added into the vials, it gradually releases a certain amount of protons (H^+) which will attack and then replace the Bu_4N^+ counterions that used to cover the POM clusters. For the macroiniator, no obvious change was observed when Bu_4N^+-POM was altered into H^+-POM in the solution, as shown in Figure 6A. However, this cation exchange process tunes the hybrid polymer $(Bu_4N)^+$-POM-PS

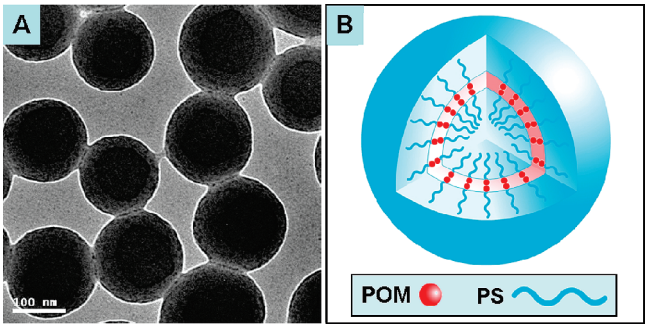

Figure 7. (A) TEM image of the hybrid vesicles. (B) Suggested structure of the hybrid vesicles.

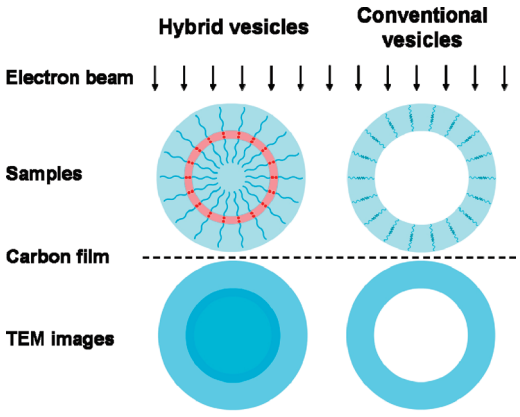

Figure 8. Schematic explanations of the difference between hybrid and conventional vesicles when viewed under TEM.

into a giant amphiphile H^+-POM-PS composed of a hydrophilic H^+-POM headgroup and a long, hydrophobic PS tail. Immediately, individual molecules self-assemble into kinetically favored aggregates in organic solvent. Therefore, the solution of H^+-POM-PS becomes turbid, and the turbid layer height rises with a time evolution as shown in Figure 6B. These results unambiguously demonstrate that we have successfully applied ATRP to the synthesis of POM-PS hybrid polymer, and the long hydrophobic PS chain has significant affection to the supramolecular aggregates via self-assembly.

The hybrid aggregates of the amphiphilic H^+-POM-PS in DMF were further explored by TEM in Figure 7A. The TEM result undoubtedly represents the aggregates consisting of a dark core, bright shell, and darker, thin ring at the interface between the core and shell. The appearance of the dark ring indicates that most POM clusters are located in the middle of the membrane which forms the vesicle, as shown in Figure 7A. The transformation from individual molecules to vesicles is a kinetically controlled process caused by the gathering of H^+-POM clusters to avoid their interaction with solvent. And because of the rapid assembly of H^+-POM-PS, some small reversed micelles might be trapped in the PS shell or/and inside the vesicles. This is the reason why some tiny dark spots can be seen in the TEM image. Finally, it is worth mentioning that the hybrid vesicle feature appeared in our TEM images is totally different from those of vesicles formed by conventional block copolymers. This difference is schematically explained in Figure 8. Clearly, the POMs gathering in the middle of the membrane and the strong electron contrast between POMs and polymers create such special image feature. The profound effects of the cation POM clusters on the morphology and chemical and physical properties of supramolecular assemblies of the hybrid polymer are in progress.

Conclusions

In summary, we have successfully applied ATRP to the construction of novel POM−polymer hybrids. As an example, based on the synthesis of POM-functionalized macroinitiator, well-defined POM−PS was created via in situ ATRP. This reaction is mild and convenient. The products, with 100% POM functionality and well-defined structure, are unique model compounds to explore the properties and understand the nature of POM−polymer hybrids. GPC observation reveals that the POM head significantly increases the overall hydrodynamic volume of the POM−PS hybrid polymer. The facile synthetic method for the functionalization of POMs, which is covalently linked to the polymerizable groups, presented here can be further extended to other polymers. By means of the cation exchange process, a novel giant amphiphile H^+-POM-polymer self-assemble in selective solvent to give anticipated hybrid vesicles. Definitely, these hybrid polymers are ideal models to understand the fundamentals of the self-assembly of hybrids in solution. Other results concerning the unusual hierarchical self-assembly behavior of these model compounds in solution will be discussed in later publications.

Experimental Section

Materials. *N*,*N*,*N*′,*N*′,*N*″-Pentamethyldiethylenetriamine (PMDETA) (99%), 2-bromoisobutyryl bromide (BIB) (98%), and tris(hydroxymethyl)aminomethane (Tris) (99.8%) were purchased from Aldrich and used without further purification. Other reagents were purchased from major chemical suppliers and used as received unless otherwise noted. Ethylene glycol (EG) was purified by distillation, dried, and redistilled. Triethylamine (TEA) was refluxed with acetic anhydride, then distilled, dried, and redistilled. Styrene (St) was stirred overnight over CaH_2 and vacuum-distilled prior to use. Cu(I)Br was purified by stirring in glacial acetic acid overnight, filtering, and washing with dry ethanol. *N*,*N*-Dimethylformamide (DMF), dichloromethane (CH_2Cl_2), and other organic solvents were dried, distilled, and kept in the presence of 4 Å molecular sieve to eliminate any traces of water before use. A strongly acidic cation-exchange resin with sodium sulfonatetype structure and spherical morphology (Dowex H^+ 50W-X2) was used in this work. The charged form of the resin was reversed from Na^+ to H^+ by treatment with 10 wt % HCl solution. Then the resin derivatives were washed well with deionized water and dried under vacuum.

Instrumentation. (i) ^{31}P NMR spectra was recorded in d_3-acetonitrile (CD_3CN). ^1H NMR spectra was recorded in *d*-chloroform ($CDCl_3$), deuterium oxide (D_2O), and d_7-*N*,*N*-dimethylformamide (d_7-DMF) on a NMR spectrometer (Varian UNITY Plus-400). (ii) The molecular mass of compounds **3** and **4** was taken on ESI-TOF mass spectrometer (X7 ICP-MS). (iii) Infrared spectra (IR) were taken on a FT-IR spectrometer (Bio-Rad FTS-135). (iv) Gel permeation chromatography (GPC) was performed by a set of a Waters 510 HPLC pump, a Waters 410 refractive index detector, and PL gel chromatography columns. DMF was used as an eluent at a flow rate of 1.0 mL/min at 45 °C. Polystyrene standards were used for the calibration. (v) Transmission electron microscopy (TEM) observations were performed by using a TEM microscope (Philips T20ST) operated under an acceleration voltage of 200 kV. A drop of solution was spread on a copper grid, and the excess solution was blotted with filter paper. Then the grids were dried under vacuum.

Synthesis of $(Bu_4N)_5[H_4P_2W_{15}V_3O_{62}]$ Cluster. According to the method reported in ref 26, we have synthesized the $(Bu_4N)_5[H_4P_2W_{15}V_3O_{62}]$ cluster. The high-sensitivity ^{31}P NMR spectrum, Figure 2A, shows only two types of phosphorus

resonances, expected for $(Bu_4N)_5[H_4P_2W_{15}V_3O_{62}]$ cluster, thereby confirming the homogeneity of the sample. The peaks at −13.11 and −7.44 ppm are assigned to the PO_4^{3-} groups connected to the W_3 cap and V_3 cap, respectively. The IR spectrum for this compound is included in Figure 4A.

Synthesis of Compound 2. A solution of EG (43 g, 0.69 mol) and TEA (8.4 g, 0.08 mol) in dry dichloromethane (250 mL) was placed into the flame-dried two-neck round-bottom flask equipped with a condenser, a dropping funnel, N_2 inlet/outlet, and a magnetic stirrer. After cooling to 0 °C, compound **1** (15 g, 0.069 mol) in dry dichloromethane (50 mL) was then added in a dropwise manner to the stirred solution. The reaction mixture was stirred at room temperature under nitrogen for 24 h and filtered to remove precipitates, and the solvent was evaporated under vacuum. The product was washed with 2 mol/L HCl solution (3 × 100 mL), and the lower, light-yellow organic phase was separated. After the water phase was extracted with chloroform (3 × 100 mL), the two organic portions were combined, diluted with dichloromethane, dried over anhydrous magnesium sulfate, and filtered. Then compound **2** was purified by silica gel column chromatography with mobile phase of petroleum ether: ethyl acetate (6:1, v/v). ^{1}H NMR ($CDCl_3$): δ = 1.956 (s, 6H, $-C(CH_3)_2Br$), 3.886 (t, 2H, $HOCH_2CH_2O-$), 4.318 (t, 2H, $HOCH_2CH_2O-$).

Synthesis of Compound 3. A solution of Tris (1.147 g, 9.48 mmol), compound **2** (2 g, 9.48 mmol), and K_2CO_3 (1.4171 g, 10.27 mmol) in dry DMF (15 mL) was placed into the round-bottom flask equipped with a condenser and a magnetic stirrer. After heating the solution to 70 °C for 24 h under argon, it was evaporated under vacuum and purified by silica gel column chromatography with mobile phase of petroleum ether: ethyl acetate (1:2, v/v). ^{1}H NMR ($CDCl_3$): δ = 2.015 (s, 6H, $-C(CH_3)_2Br$), 3.872 (s, 6H, $(HOCH_2)_3C-$) (Figure 3A). MS spectrum (ESI, calculated: 269.03 and 271.02 g/mol; found: 292.0153 and 294.0136 g/mol ($M + Na^+$)).

Synthesis of Bu_4N^+-POM-Tris-BIB (4). $(Bu_4N^+)_5[H_4P_2W_{15}V_3O_{62}]$ (1 g) was added to a solution of compound **3** (0.0625 g) in DMF (13.5 mL). After heating the solution to 70 °C for 7 days under argon, it was cooled and added in a dropwise manner at 25 °C to stirred Et_2O (150 mL), and the resulting yellow solid collected and redissolved in the minimum volume of MeCN. After filtration, the product was reprecipitated by addition of ethoxyethane. This procedure was repeated twice, and the resulting yellow powder was washed with ethoxyethane and dried under vacuum at 50 °C for 2 days. The ^{1}H NMR (in d_7-DMF), IR, and MS (ESI) spectra of Bu_4N^+-POM-Tris-BIB are included in Figure 3B, Figure 4B, and Figure S5, respectively. In Figure 3B the peak at 5.7 ppm assigned to methylene protons in Tris indicates the successful linking between hydrophilic anionic POM clusters and hydrophobic polymers.

Synthesis of Bu_4N^+-POM-PS (5). A typical ATRP was carried out as follows: in a dried Schlenk flask, St (4.6456 g, 44.7 mmol), compound **4** (0.1842 g, 0.034 mmol), and DMF (6 mL) were added. After three freeze−pump−thaw cycles, PMDETA (23.5 mg, 0.136 mmol) and Cu(I)Br (9.8 mg, 0.068 mmol) were added under N_2. After stirring for 10 min at room temperature (RT), the flask was placed in a thermostated oil bath at 110 °C. The polymerization was stopped by cooling to room temperature and opening the flask to air. The mixture was then diluted in 10 mL of DMF and passed through neutral alumina column. The final pure product was obtained after precipitating in MeOH. From the integral value of aromatic (I_{Ar}) and hydroxymethyl protons ($I_{5.6}$), $\overline{M}_n$ can also be calculated according to the equation

$$\overline{M}_{n,PS}(^1\text{H NMR}) = \frac{6I_{Ar}}{5I_{5.6}} \times 104 \quad (1)$$

by ^{1}H NMR (Figure 3C), and it agrees well with the GPC result. The number, 104, is the molecular weight of styrene monomer. The ^{1}H NMR (in d_7-DMF) and IR spectra of Bu_4N^+-POM-PS are included in Figure 3C and Figure 4C, respectively. GPC (DMF, eluent): $\overline{M}_n$ = 119 000 g/mol, PDI = 1.81.

Acknowledgment. This work was supported by National Natural Science Foundation of China (20734001).

Supporting Information Available: Detailed characterization data. This material is available free of charge via the Internet at http://pubs.acs.org.

References and Notes

(1) *Polyoxometalate Chemistry—from Topology via Self-assembly to Applications*; Pope, M. T., Muller, A., Eds.; Kluwer Academic Publishers: Dordrecht, 2001.
(2) Special thematic issue on polyoxometalates: *Chem. Rev.* **1998**, *98*.
(3) Rhule, J. T.; Hill, C. L.; Judd, D. A.; Schinazi, R. F. *Chem. Rev.* **1998**, *98*, 327.
(4) Hasenknopf, B. *Front. Biosci.* **2005**, *10*, 275.
(5) Judd, D. A.; Nettles, J. H.; Nevins, N.; Snyder, J. P.; Liotta, D. C.; Tang, J.; Ermolieff, J.; Schinazi, R. F.; Hill, C. L. *J. Am. Chem. Soc.* **2001**, *123*, 886.
(6) Shigeta, S.; Mori, S.; Kodama, E.; Kodama, J.; Takahashi, K.; Yamase, T. *Antiviral Res.* **2003**, *58*, 265.
(7) Wang, X. H.; Liu, J. F.; Pope, M. T. *Dalton Trans.* **2003**, 957.
(8) Yanagie, H.; Ogata, A.; Mitsui, S.; Hisa, T.; Yamase, T.; Eriguchi, M. *Biomed. Pharmacother.* **2006**, *60*, 349.
(9) Gouzerh, P.; Proust, A. *Chem. Rev.* **1998**, *98*, 77.
(10) Sanchez, C.; Soler-Illia, G. J. A. A.; Ribot, F.; Lalot, T.; Mayer, C. R.; Cabuil, V. *Chem. Mater.* **2001**, *13*, 3061.
(11) Alam, M. A.; Kim, Y.-S.; Ogawa, S.; Tsuda, A.; Ishii, N.; Aida, T. *Angew. Chem., Int. Ed.* **2008**, *47*, 2070.
(12) (a) Li, H. L.; Qi, W.; Li, W.; Sun, H.; Bu, W. F.; Wu, L. X. *Adv. Mater.* **2005**, *17*, 2688. (b) Li, H. L.; Sun, H.; Qi, W.; Xu, M.; Wu, L. X. *Angew. Chem., Int. Ed.* **2007**, *46*, 1300.
(13) (a) Kurth, D. G.; Lehmann, P.; Volkmer, D.; Cölfen, H.; Koop, M. J.; Muller, A.; Du Chesne, A. *Chem.—Eur. J.* **2000**, *6*, 385. (b) Volkmer, D.; Du Chesne, A.; Kurth, D. G.; Schnablegger, H.; Lehmann, P.; Koop, M. J.; Muller, A. *J. Am. Chem. Soc.* **2000**, *122*, 1995. (c) Volkmer, D.; Bredenkötter, B.; Tellenbröker, J.; Kögerler, P.; Kurth, D. G.; Lehmann, P.; Schnablegger, H.; Schwahn, D.; Piepenbrik, M.; Krebs, B. *J. Am. Chem. Soc.* **2002**, *124*, 10489.
(14) Judeinstein, P. *Chem. Mater.* **1992**, *4*, 4.
(15) (a) Mayer, C. R.; Cabuil, V.; Lalot, T.; Thouvenot, R. *Angew. Chem., Int. Ed.* **1999**, *38*, 3672. (b) Mayer, C. R.; Thouvenot, R.; Lalot, T. *Chem. Mater.* **2000**, *12*, 257. (c) Mayer, C. R.; Thouvenot, R.; Lalot, T. *Macromolecules* **2000**, *33*, 4433.
(16) (a) Proust, A.; Thouvenot, R.; Gouzerh, P. *Chem. Commun.* **2008**, 1837. (b) Xu, L.; Lu, M.; Xu, B.; Wei, Y.; Peng, Z.; Powell, D. R. *Angew. Chem., Int. Ed.* **2002**, *41*, 4129. (c) Peng, Z. H. *Angew. Chem., Int. Ed.* **2004**, *43*, 930.
(17) Moore, A. R.; Kwen, H.; Beatty, A. B.; Maatta, E. A. *Chem. Commun.* **2000**, 1793.
(18) (a) Bareyt, S.; Piligkos, S.; Hasenknopf, B.; Gouzerh, P.; Lacôte, E.; Thorimbert, S.; Malacria, M. *Angew. Chem., Int. Ed.* **2003**, *42*, 3404. (b) Bareyt, S.; Piligkos, S.; Hasenknopf, B.; Gouzerh, P.; Lacte, E.; Thorimbert, S.; Malacria, M. *J. Am. Chem. Soc.* **2005**, *127*, 6788. (c) Li, J.; Huth, I.; Chamoreau, L.-M.; Hasenknopf, B.; Lacte, E.; Thorimbert, S.; Malacria, M. *Angew. Chem., Int. Ed.* **2009**, *48*, 2035.
(19) Hou, Y.; Hill, C. L. *J. Am. Chem. Soc.* **1993**, *115*, 11823.
(20) Zeng, H. D.; Newkome, G. R.; Hill, C. L. *Angew. Chem., Int. Ed.* **2000**, *39*, 1772.
(21) (a) Song, Y. F.; Long, D. L.; Cronin, L. *Angew. Chem., Int. Ed.* **2007**, *46*, 3900. (b) Song, Y. F.; McMillan, N.; Long, D. L.; Thiel, J.; Ding, Y. L.; Chen, H. S.; Gadegaard, N.; Cronin, L. *Chem.—Eur. J.* **2008**, *14*, 2349. (c) Pradeep, C. P.; Long, D. L.; Newton, G. N.; Song, Y. F.; Cronin, L. *Angew. Chem., Int. Ed.* **2008**, *47*, 4388.
(22) Favette, S.; Hasenknopf, B.; Vaissermann, J.; Gouzerh, P.; Roux, C. *Chem. Commun.* **2003**, 2664.

(23) Wang, J. S.; Matyjaszewski, K. *J. Am. Chem. Soc.* **1995**, *117*, 5614.
(24) Matyjaszewski, K.; Xia, J. H. *Chem. Rev.* **2001**, *101*, 2921.
(25) Kamigaito, M.; Ando, T.; Sawamoto, M. *Chem. Rev.* **2001**, *101*, 3689.
(26) Finke, R. G.; Rapko, B.; Saxton, R. J.; Domaille, P. J. *J. Am. Chem. Soc.* **1986**, *108*, 2947.
(27) Newkome, G. R.; Yao, Z.-Q.; Baker, G. R.; Gupta, V. K. *J. Org. Chem.* **1985**, *50*, 2003.
(28) Newkome, G. R.; Baker, G. R.; Arai, S.; Saunders, M. J.; Russo, P. S.; Theriot, K. J.; Moorefield, C. N.; Rogers, L. E.; Miller, J. E.; Lieux, T. R.; Murray, M. E.; Phillips, B.; Pascal, L. *J. Am. Chem. Soc.* **1990**, *112*, 8458.